Quantitative EPR Spin Trapping. 1. Nitrogen Dioxide Radicals and Nitrite Ions from Energetic Materials in Alkaline Aqueous Solution

M. D. Pace*

Code 6120, Naval Research Laboratory, 4555 Overlook Avenue, S.W., Washington, D.C. 20375-5342

A. J. Carmichael

Armed Forces Radiobiology Research Institute, Betheseda, Maryland 20889-5603

Received: May 30, 1996; In Final Form: December 27, 1996[⊗]

A new application of electron paramagnetic resonance (EPR) spin trapping is described using the nitromethane *aci* anion ($CH_2{=}NO_2^-$) spin trapping technique for quantitative measurement of nitrogen dioxide radicals ($^{\bullet}NO_2$) and nitrite ions (NO_2^-) in strong alkaline aqueous solution. The relative concentration of a spin adduct radical, dinitromethyl dianion radical [$^-O_2N{-}CH{=}NO_2^{\bullet -}$] (**I**), produced by ultraviolet photolysis, is shown to be proportional to the concentration of NO_2^- dissolved in alkaline solution. This method is applied to estimate the $^{\bullet}NO_2$ concentrations produced by decomposition of two energetic nitramine compounds: cyclotrimethylenetrinitramine, $C_6H_6N_6O_6$ (RDX), and ammonium dinitramide, $NH_4^+N(NO_2)_2^-$ (ADN), by using calibration plots of the spin concentration of **I** versus time of photolysis. Calibrations were prepared using sodium nitrite ($NaNO_2$) or ammonium nitrate (NH_4NO_3) which behave similarly to the energetic compounds with respect to formation of **I**.

Introduction

The recent trend toward demilitarization has focused attention on the destruction and disposal of energetic materials stockpiles. New routes to the disposal of energetic materials are needed which will decompose these materials without producing environmental pollution. Nonpolluting disposal methods are also part of the strategy of life cycles of new energetic materials which seeks to completely recycle explosives without generating toxic or environmental pollutants. Chemical decomposition of energetic nitramine compounds by alkaline aqueous hydrolysis is a laboratory method which has potential for large scale application.

Synthesis studies have shown that alkaline solutions of hydroxyl ions (OH^-) decompose nitramine explosives such as RDX (cyclotrimethylenetrinitramine).[1] More recent studies have shown that strong alkaline solutions dissociate the nitro groups of nitramine compounds into nitrite ions (NO_2^-).[2] For example, in a solution having an hydroxyl ion concentration of *ca.* 10^{-2} mol L^{-1}, RDX decomposes according to eq 1, forming a ring

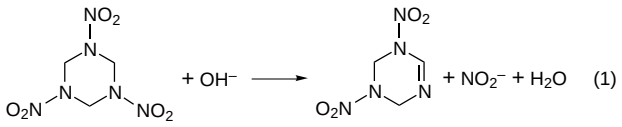

(1)

intact intermediate (1,3,5-triaza-3,5-dinitrocyclohex-1-ene) and nitrite ion. This decomposition involves abstraction of a methylene proton by OH^- followed by elimination of nitrite ion with formation of nitrous acid. In strongly basic solution, the concentration of hydroxyl ions increases with increasing alkalinity of solution, producing higher concentrations of the NO_2^- ion as an initial decomposition product of RDX and similar nitramines.[3] This suggests that the extent of decomposition of nitramines by alkaline hydrolysis can be determined by detection and quantification of the nitrite ion concentration.

The NO_2^- generated in the decomposition of nitramines is important because it is related by chemistry to most other reactive nitrogen intermediates (RNI). These include $^{\bullet}NO_2$, $^{\bullet}NO$, and NO_3^-. Most RNI can be interconverted to one another given the right set of conditions. For instance, the formation of nitric oxide ($^{\bullet}NO$), nitrogen dioxide ($^{\bullet}NO$), nitrites (NO_2^-), and nitrates (NO_3^-) as direct decomposition products of high-energy nitramines or as secondary decomposition products of these high-energy compounds may have a large environmental impact (acid rain, depletion of ozone). These are additional reasons why the mechanism of decomposition of high-energy nitramines is important.

The detection of nitrite ions in aqueous solution is usually accomplished by colorimetric reactions such as the Griess reaction, which forms a pink azo dye by reaction of nitrite ions with *N*,*N*-dimethyl-1-naphthylamine and sulfanamide.[4] Although this method or spectroscopic methods such as LC/MS (liquid chromatography/mass spectroscopy) or ultraviolet absorption (UV/vis) spectroscopy are useful for analysis of final products, such analyses do not give the intermediates which lead to final products. Electron paramagnetic resonance (EPR) spin trapping is a method for detecting intermediate free radical molecules.[5] It consists of reacting short-lived free radicals with a spin trap, yielding a longer-lived nitroxide spin adduct which can be identified by EPR.

The objective of this paper is to demonstrate a method by which EPR spin trapping experiments can be used to measure the concentration of nitrogen dioxide radicals ($^{\bullet}NO_2$) originating from the photodecomposition of high-energy compounds (RDX) and/or from nitrite ions (NO_2^-) in strong alkaline aqueous solution.[6] Since UV radiation of NO_2^- yields $^{\bullet}NO_2$, and preliminary data suggest that the concentration of $^{\bullet}NO_2$ formed is proportional to the initial concentration of NO_2^-, therefore, the method described in this report deals with the determination of both species.[7] Furthermore, NO_2^- solutions of known concentrations can be used as standards for the decomposition of high-energy materials. In conventional spin trapping studies, nitrone or nitroso compounds are used as the spin traps. In the

[⊗] Abstract published in *Advance ACS Abstracts,* February 15, 1997.

S1089-5639(96)01578-2

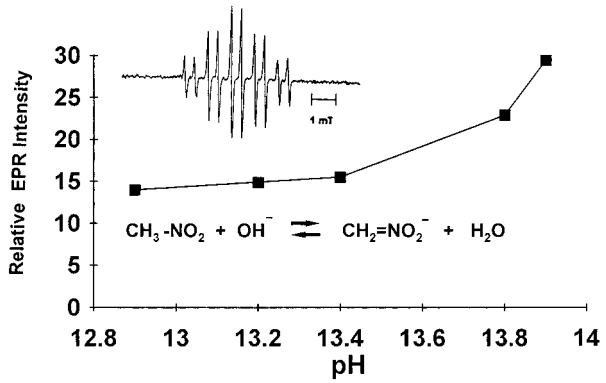

Figure 1. EPR spectrum of the dinitromethyl dianion radical shown in eq 1 and the pH dependence of the relative integrated signal intensity for the pH range of these experiments from pH = 12.8 to ca. 13.8. The signal varies by a factor of 2 in this pH range.

present study, a new type of spin trapping using nitromethane as the quantitative spin trapping agent is described.[8] Although we have previously reported qualitative application of EPR/nitromethane spin trapping to study nitramine decomposition by UV photolysis of nitramines in alkaline solution, this is the first attempt to quantitate this new type of spin trapping. Other results of nitromethane spin trapping have also recently been reported.[9] Application to energetic materials is demonstrated by measuring $^{\bullet}NO_2/NO_2^-$ concentrations from photodecomposition of RDX and ammonium dinitramide (ADN) in alkaline solutions. This has potential application in evaluation of catalysts designed to decompose waste explosives and propellants.

Experimental Section

Sodium nitrite ($NaNO_2$) (Aldrich, 97+%), sodium hydroxide (NaOH) (Aldrich), nitromethane (CH_3NO_2) (Aldrich, 99+%), and ammonium nitrate (NH_4NO_3) (Aldrich) were purchased. RDX and ADN [$NH_4^+N(NO_2)_2^-$] were received from the Naval Ordnance Center, Indian Head, MD. Alkaline H_2O solution was prepared using sodium hydroxide pellets dissolved in deionized H_2O (18 mΩ) or by using 10 N NaOH diluted to required concentrations. The pH values of alkaline solutions were kept within the range $12.9 < pH < 13.9$. This is important for quantitative work because the concentration of a radical adduct between nitromethane *aci* anion and nitric oxide ($^{\bullet}NO$) has been shown to increase with increasing pH.[10] In this study, the detected EPR signal is due to an adduct of nitrogen dioxide radical ($^{\bullet}NO_2$) and the nitromethane *aci* anion ($CH_2{=}NO_2^-$) to give dinitromethyl dianion radical (**I**).

$$CH_2{=}NO_2^- + {}^{\bullet}NO_2 \longrightarrow {}^-O_2N{-}CH{=}NO_2^{\bullet -} \qquad (2)$$

nitromethane *aci* anion — **I** — dinitromethyl dianion radical

The EPR spectrum of radical **I** and pH dependence of the EPR signal intensity are shown in Figure 1. The integrated EPR signal intensity of **I** varies by a factor of 2 between pH 12.9 and pH 13.9. Below pH 12, EPR signals of **I** were not detected.

Quantitative measurements required the following steps: (i) Solutions having known concentrations of nitrite ions were prepared using $NaNO_2$ in basic aqueous solution at constant pH. (ii) EPR spectra of **I** for each solution plus added spin trap were recorded versus time of photolysis. (iii) The resulting EPR spectra were double integrated, and the integrals were plotted versus time of photolysis. Alternatively, the signal intensities of the two most intense peaks of the spectrum of **I** can be plotted versus time of photolysis. (iv) Data points taken from step iii were used to produce calibration plots of the relative EPR signal intensities of **I** for different photolysis times versus initial nitrite ion concentrations of each solution.

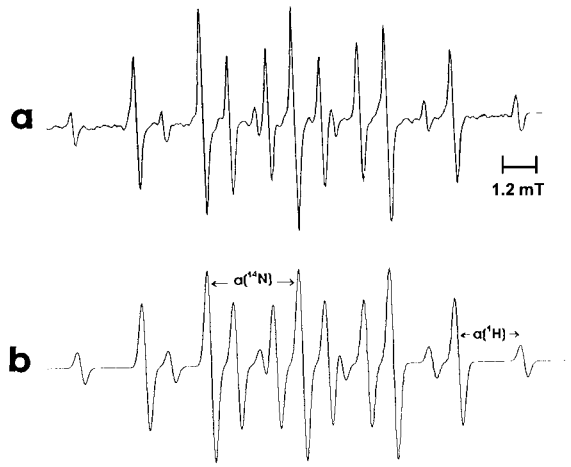

Figure 2. EPR "artifact" signals from UV photolysis of nitromethane (25 μL) in alkaline NaOH solution (pH $\sim$ 13). (a) The experimental "artifact" EPR spectrum. This signal was usually observed in conjunction with ADN samples. (b) One possible assignment of the spectrum with the simulated first-derivative EPR spectrum of (a) having one ^{14}N hyperfine coupling with $a(^{14}N) = 1.675$ mT and four equivalent ^1H hyperfine couplings with $a(^1H) = 1.2$ mT. Another possible assignment is to two overlapped spectra.

Calibration solutions are described as follows. $NaNO_2$ was added to 2 mL of alkaline solution, giving a stock concentration of 0.45 mol L^{-1} (M) in $NaNO_2$. All solutions were studied under aerated conditions. Dilutions of the stock solution were carried out using alkaline H_2O to give a set of solutions labeled as A, B, C, D having $NaNO_2$ concentrations of $A = 0.450$ M, $B = 0.227$ M, $C = 0.113$ M, and $D = 0.057$ M. Note that in these examples each successive solution was diluted by a factor of $^1/_2$. The concentration of $CH_2{=}NO_2^-$ spin trap of each solution was 25 μL (4.6×10^{-4} mol)/mL. Immediately after adding the spin trap, a 150 μL portion of $NaNO_2$ solution containing the spin trap solution was loaded into a quartz flat cell (Wilmad WG-812), and the cell was inserted into a Bruker TE_{102} cavity. In situ ultraviolet (UV) photolysis was carried out in the EPR cavity. The ultraviolet light intensity was kept constant for each experiment, and a monochromator was used to restrict light to 360 nm or greater wavelengths. This produced the EPR signal of the dinitromethyl radical anion (**I**) (eq 2).[7] We note that other EPR signals of free radicals from photolysis of nitromethane in alkaline aqueous solution (without added $NaNO_2$) were sometimes detected. The experimental EPR spectrum of this "artifact" radical is shown in Figure 2a,b. The spectrum does not coincide with that of the nitromethane anion radical ($CH_3{-}NO_2^{\bullet -}$) which has been reported under similar conditions.[8] With 360 nm UV light and high pH, the artifact radical signals disappear, and the major EPR signal is due to **I**, the radical adduct spectrum of $CH_2{=}NO_2^-$ and $^{\bullet}NO_2$.

For quantitative measurements, experimental spectra were recorded as first-derivative spectra using a Bruker ER 200 spectrometer or a Varian X-band spectrometer. The spectrometer settings were kept constant. Spectrometer settings were as follows: a magnetic field of 345.5 mT (10 G = 1 mT); a microwave power of 20 mW; a gain of 6.3×10^4; a time constant of 0.1 s; a sweep width of 8 mT; a magnetic field modulation of 0.08 mT (100 kHz). Spectra were slightly overmodulated to improve signal-to-noise ratio. In computer-acquired spectra, a sweep time of 20 s was used, with three

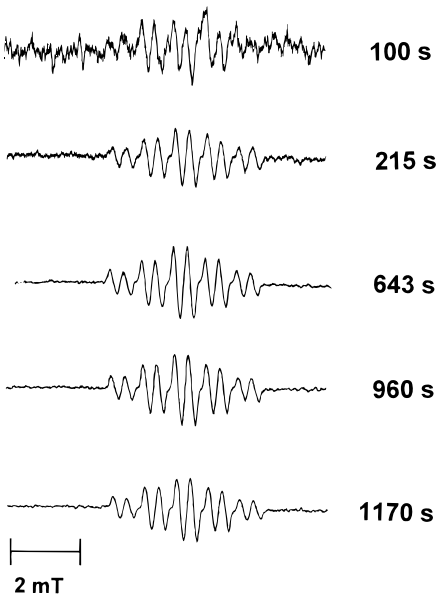

Figure 3. Using solution A, described in the Experimental Section, a first-derivative EPR spectrum of radical **I** ($^{-}O_2N-CH{=}NO_2^{\bullet-}$) at different times from the start of UV photolysis was recorded as shown. Each spectrum is normalized to the most intense peak. The hyperfine splittings of this spectrum are $a(^{14}N) = 0.96$ mT for two equivalent ^{14}N hyperfine couplings and $a(^{1}H) = 0.42$ mT for one ^{1}H hyperfine coupling. The signal intensity increases up to ca. 643 s as indicated by the signal-to-noise ratio.

TABLE 1: EPR Spectral Integrations of Solution A

time (s)	rel concn[a]	spin concn[b]
100	0.14	4.5×10^{14}
215	0.41	1.3×10^{15}
643	0.98	3.2×10^{15}
960	1.00	3.3×10^{15}
1170	0.95	3.1×10^{15}

[a]Relative integrated intensities of spectra in Figure 3. Units are arbitrary. [b] Probable error of the spin concentration estimated as $\pm 0.6 \times 10^{15}$ spins.

scans averaged per spectrum, giving a total time of spectral acquisition as ca. 60 s per spectrum. In experiments using the chart recorder, kinetic data were recorded by scanning the two major peaks of an EPR spectrum of **I** at 10 s intervals. Interpretation and comparison of EPR spectra are demonstrated by the set of spectra given in Figure 3 for solution A.

EPR spectra of radical **I** are given in Figure 3 corresponding to different times from the start of photolysis of solution A. For these spectra, the *Y* axes are normalized to the most intense peak. The increase of signal strength from 100 to 643 s is apparent from the relative values of the integrated intensities, indicated in Table 1, and from the improvement in signal-to-noise ratios. Each experimental first-derivative spectrum was double integrated. Spectral integrations were performed using SUMSPEC computer programs developed by the Biophysics Research Institute, Medical College of Wisconsin.[11] Instrument and light settings were constant throughout each experiment, allowing for quantitative comparisons of spin concentrations. Absolute concentrations were obtained by comparisons of relative spin concentrations to a standard. For this study di-*tert*-butyl nitroxide radical in H_2O was used as as a spin standard diluted to a concentration of 6.88×10^{-4} M or 6.12×10^{16} spins per flat cell volume of 150 μL. Table 1 gives spin concentrations of the spectra in Figure 3.

As a second measurement, NO_2^- concentrations were also measured by UV absorption spectroscopy prior to spin trapping. UV absorption spectra of nitrite ions in aqueous solution show

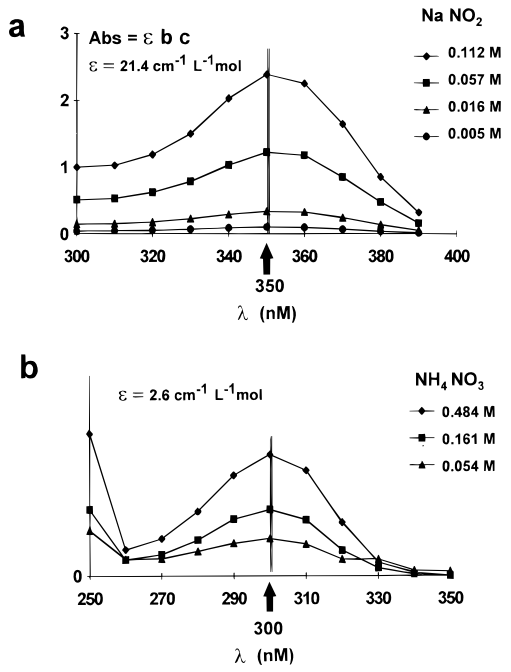

Figure 4. UV absorption spectra of (a) $NaNO_2$ in alkaline solution having a maximum absorbance at 360 nm and (b) NH_4NO_3 having a maximum absorbance at 300 nm.

an absorption peak at ca. 350 nm. The 350 nm peak was used for comparative measurements of NO_2^- concentrations using Beer's law relationship $A = \epsilon bc$, where A is the absorbance, ϵ is the molar absorptivity which was determined as $\epsilon_{350} = 2.14 \times 10^4$ mol^{-1} cm^2, $b = 1$ cm, and c is the NO_2^- concentration (mol L^{-1}). UV/vis absorption data of $NaNO_2$ (300−390 nm) and NH_4NO_3 (250−350 nm) are given in Figure 4, a and b, respectively. The standard plotting program, ORIGIN, was used to fit all sets of points whenever necessary.

Results

Nitromethane *Aci* Anion. There are several mechanisms involving RNI that yield $^{\bullet}NO_2$, which is ultimately trapped by *aci*-nitromethane.[9,12] This spin trapping method does not distinguish between these various pathways to formation of $^{\bullet}NO_2$ but responds to the overall yield of $^{\bullet}NO_2$. A predominant pathway to formation of $^{\bullet}NO_2$ in these studies is from NO_2^-. This spin trapping method is quantitative for measuring NO_2^- because formation of NO_2^- is the first step in the base hydrolysis of nitramines.[3]

In alkaline solution nitromethane *aci* anion is produced by the following equilibrium.

$$CH_3{-}NO_2 + OH^- \leftrightarrows CH_2{=}NO_2^- + H_2O \qquad (3)$$

For strong alkaline solution (pH ∼ 13) the equilibrium is shifted to the right-hand side of eq 3. As given in eq 2, the EPR spin trapping signal detected during photolysis of nitrite ions in aqueous solution is an adduct of nitromethane *aci* anion and nitrogen dioxide radical ($^{\bullet}NO_2$).

The following results show that the spin concentration of **I** is proportional to the NO_2^- concentration in alkaline solution. Figure 5a gives photolysis data for the solutions labeled A, B, C, D. For each solution, the relative spin concentration of **I** is plotted versus the time of photolysis. For photolysis of up to ca. 600 s an increase of the concentration of **I** is observed. Decreases of concentrations of **I** beyond 600 s may be due to depletion of the spin trap or due to the rate of formation of **I**

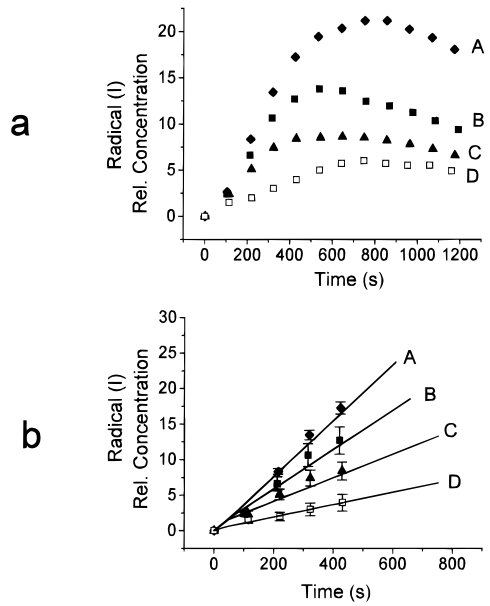

Figure 5. (a) Plots of the relative concentration of **I** versus time of photolysis are given for NO_2^- concentrations: *A* (◆) = 0.45 M; *B* (■) = 0.227 M; *C* (▲) = 0.113 M; *D* (□) = 0.057 M. Note that each successive solution was diluted by a factor of $^1/_2$. The concentration of **I** begins to decrease after ca. 500 s of photolysis. (b) Linear portions of the curves in (a) are replotted on an expanded time scale. This clearly shows that the data are approximately linear for $t < 500$ s and that the slopes of linear least square fits to the data vary in proportion to the NO_2^- concentrations.

TABLE 2: Linear Fits to $NaNO_2$ Calibration Data

solution	N^a	m^b	b^b	SD^c
A	6	0.0393	−0.24	1.12
B	6	0.0276	0.36	1.22
C	4	0.0225	−0.02	0.19
D	5	0.0093	0.00	0.06

[a] Number of points. [b] From equation "$y = mx + b$" describing a straight line. [c] Standard deviation.

equaling the the rate of decomposition of the adduct. Points from Figure 5a showing increases of intensity are replotted in Figure 5b.

Linear regression fits to the data are shown in Figure 5b, and equations of these lines are given in Table 2. From Table 2 note that the slopes decrease in the order A > B > C > D. A basis for quantitative measurement is that slopes vary in proportion to the concentration of NO_2^- in solution. That is, the decreasing concentration of NO_2^- from A to D is reflected by proportional decreases of the slopes. Although the data plots in Figure 5b are suitable standard curves, data in Figure 5b may be displayed in more convenient calibration plots.

A calibration plot for each different solution is made by plotting the NO_2^- concentration (known from experimental preparation) versus the relative concentration of **I** *at a particular time of photolysis* for each different solution. Such a plot is shown in Figure 6a, giving a direct correlation between the NO_2^- concentration of each solution and the relative concentrations of **I**. This plot shows that, for a constant time of photolysis, the concentration of **I** increases with increasing NO_2^- concentration or, conversely, that for a given NO_2^- concentration the concentration of **I** increases with increasing time of photolysis. A log−log plot as shown in Figure 6b simplifies direct *X* versus *Y* comparisons. The plot in Figure 6b provides a graph for determining an unknown NO_2^- concentration simply by measuring the relative concentration of radical **I** under identical instrument and UV light conditions as used to generate

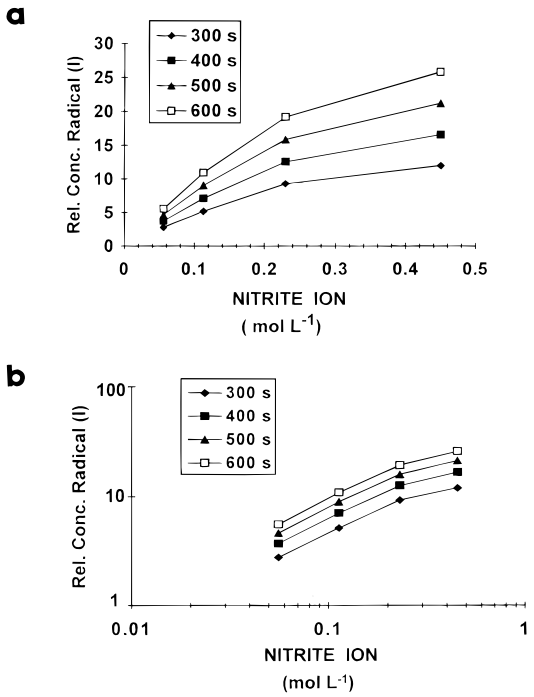

Figure 6. (a) This plot represents calibration curves of the relative concentration of **I** versus the starting concentration of solutions A, B, C, D. Points from Figure 5a for selected times, 300, 400, 500, and 600 s, are plotted. (b) Data in (a) are replotted on a log−log scale giving plots which may be used for determining an "unknown" NO_2^- concentration.

the calibration data. The range of concentrations for Figure 6 is from 0.04 to 0.5 M; however, curves can be developed for lower or higher ranges of NO_2^- concentrations.

To illustrate this method, a test solution of $NaNO_2$ having an NO_2^- concentration of 0.145 M was prepared separately from the calibration solutions and then treated by the *aci*-nitromethane spin trapping method. A 150 μL portion of the test solution was UV irradiated in situ in the EPR cavity, and spectra were recorded versus time as shown in Figure 7a. Radical adduct relative concentrations of **I** (denoted as *S* and expressed in arbitrary units), measured from Figure 7a, are $S = 4.5$ for $t = 300$ s, $S = 6.3$ for $t = 400$ s, $S = 9.2$ for $t = 500$ s, and $S = 12.0$ for $t = 600$ s. These times of photolysis were arbitrarily chosen for convenience.

These values are replotted in the log−log plot of Figure 7b and are indicated by the arrow in Figure 7b. To locate these points on the plot, the nitromethane *aci* anion adduct concentration is measured along the *Y* axis, and a horizontal line is extrapolated to intersect the time lines for each different photolysis time. Intersections for different times of photolysis ideally fall along a single verticle line which intersects the *X* axis, giving the "unknown" concentration. In Figure 7b the lines connecting points are omitted for clarity. In this case, the point at $t = 300$ s deviates the greatest from predicted values; however, the NO_2^- concentration value of 0.13 at $t = 600$ s corresponds closely to the concentration of $NaNO_2$ for this sample, measured as 0.14 M by UV/vis. Test data were repeated for four different "unknown" $NaNO_2^-$ concentrations, and the results are given in Table 3.

Nitrite Ion Concentrations of RDX and ADN. This technique was applied to estimate the nitrite ion concentrations from RDX and ADN in alkaline solutions. Alkaline solutions of RDX or ADN were subjected to UV photolysis in the EPR cavity. At a particular time of photolysis, the NO_2^- concentration of RDX or ADN solution was estimated by comparing the

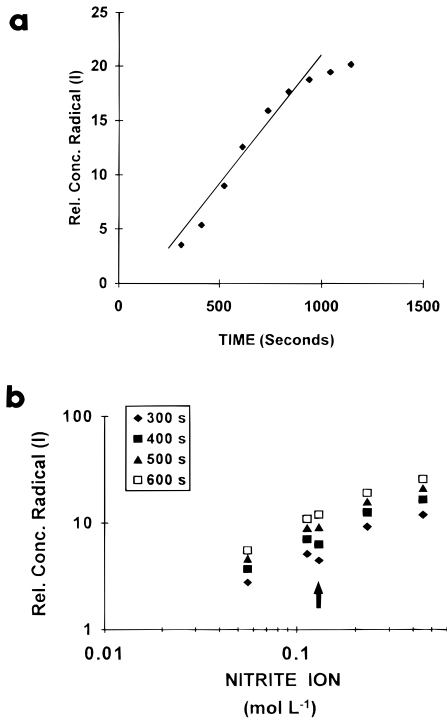

Figure 7. (a) An NO_2^- solution, different from that used to develop Figure 6, was treated by the nitromethane *aci* anion method. The data show a linear growth of **I** versus time of photolysis. Points from this curve for times 300, 400, 500, and 600 s are plotted in (b). (b) Calibration data from Figure 5b with points from (a) indicated by the arrow. Ideally, these points would fall on the calibration lines. There is good corrrespondence for $t = 600$ and 500 s. Points for $t = 400$ and 300 s show greater deviation from the linear data. The concentration determined by points at $t = 600$ and 500 s is 0.13 M (measure from the bottom of the arrow to the intersection with the X axis). This corresponds to the NO_2^- concentration as prepared by weight of $NaNO_2$ for this solution.

TABLE 3: Estimation of NO_2^- Concentrations of Test Solutions[a]

solution no.	weight (mol L^{-1})	UV/vis (mol L^{-1})	EPR (mol L^{-1})
1	0.066	0.071	0.080
2	0.014	0.016	0.020
3	0.124	0.150	0.110
4	0.007	0.010	0.008

[a] Concentrations determined by weight of $NaNO_2$ added to solution, by UV/vis absorption spectroscopy, and by the EPR spin trapping method.

spin concentration of **I** to calibration data. $NaNO_2$ calibrations were 0.112, 0.057, and 0.016 M. Figure 8 gives results for RDX, and linear fits to these data are indicated. The RDX result for this sample falls along a slope of 0.013, between the 0.057 M (slope = 0.018) and 0.016 M (slope = 0.008) lines. This directly indicates that the nitrite ion concentration is greater than 0.016 M but less than 0.057 M. From Figure 8a, values of the relative spin concentrations of **I** (arbitrary units) were determined as $S = 28.6$ at 200 s, $S = 29.9$ at 300 s, $S = 31.2$ at 400 s, and $S = 32.5$ at 500 s. A calibration plot comparing the RDX data to the $NaNO_2$ calibration data is shown in Figure 8b. From the calibration plots (Figure 8b), the concentration of NO_2^- ion estimated as occurring from RDX is *ca.* 4.4×10^{-2} mol L^{-1}.

Unlike RDX, ADN is very soluble in water (500 g/L). UV absorption experiments of ADN solutions previously exposed to ultraviolet light indicate that most of the ADN decomposes during photolysis. An alkaline ADN solution was prepared having a concentration by weight of 0.020 mol L^{-1}. The spin trapping experiment was repeated with ADN, using $NaNO_2$ as

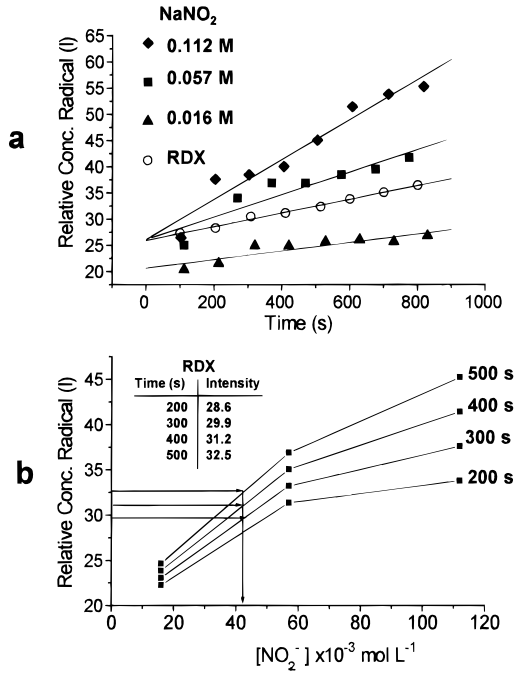

Figure 8. (a) Plot of relative concentration of **I** versus time of photolysis for RDX in alkaline solution and for three different concentrations of $NaNO_2$ in alkaline solution using the spin trapping technique described in Figures 5−7. (b) Plots of the concentration of **I** in the $NaNO_2$ solutions of (a) at times 200, 300, 400, and 500 s versus the NO_2^- concentrations of these solutions gives calibration curves. The concentration of **I** for the RDX solution is indicated by the arrows at $t = 600$ s and indicates that the NO_2^- concentration of the RDX solution was ca. 44×10^{-3} mol L^{-1}.

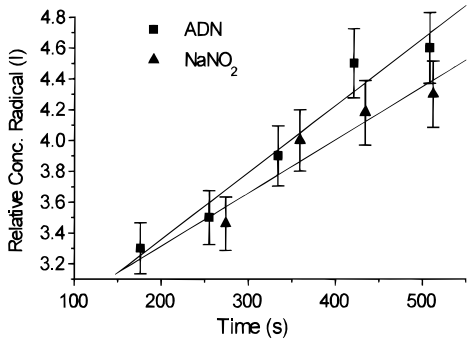

Figure 9. Plot of the concentration of **I** versus time of photolysis for alkaline solutions of $NaNO_2$ and ADN. The NO_2^- concentration of $NaNO_2$ solution was 0.022 M. The slopes of the ADN data and $NaNO_2$ data are similar, indicating that the concentrations of NO_2^- in the two solutions are similar. An estimated NO_2^- concentration of the ADN solution based on the ratio (1.2) of the slopes is 0.022 M × 1.2 = 0.026 M.

a standard. Experiments show that NH_4NO_3 may also be used as a standard for preparing calibration curves for ADN.

In this experiment, the ADN result gave data for the relative concentration of **I** very near the data set of the $NaNO_2$ calibration data (Figure 9). Therefore, the nitrite ion concentration of ADN was estimated using only one set of calibration data. The ratio of the slopes in Figure 9 is ADN:$NaNO_2$ of 0.015/0.013 = 1.2. Since the NO_2^- concentration of the $NaNO_2$ solution was 0.022 M, the ADN NO_2^- concentration estimated by the spin trapping method is 1.2 × 0.022 M = 0.026 M. The ADN concentration of this solution based on weight of ADN added to alkaline solution is 0.019 M. However, each ADN molecule contains two NO_2 groups. Therefore, comparison of ADN concentration (0.019 M) to NO_2^- concentration (0.026

M) indicates that 1.4 (0.026/0.019) NO_2^- ions are produced in solution per ADN molecule.

Discussion

As a method of qualitative detection, the EPR spin trapping method excels at characterization of free radical intermediates. The use of nitromethane *aci* anion as a qualitative spin trap has been reported for radiolysis studies in which several anionic species were studied (including NO_2^-), and the nitromethane *aci* anion method has been reported for reactions using catalysts such as TiO_2.[8] However, only recently has the nitromethane *aci* anion reaction been utilized for trapping $^{\bullet}NO_2$ produced in photolysis studies.[12] This trapping method has also been applied to trap sulfur-centered radicals from 6-mercaptopurine and other compounds.[13] In these studies the nitromethane *aci* anion method was demonstrated as a qualitative trapping method for identification of radical intermediates.

Application of spin trapping to quantitative studies is generally difficult because of very rapid free radical reaction or decay rates. In this study, quantitative measurements were feasible due to the following factors: (i) The rate of formation of **I** by UV photolysis is first-order in NO_2^-; that is, the concentration of **I** at time t is dependent on the initial concentration of NO_2^-. (ii) The decay of radical **I** is slow compared to its rate of formation. The decay of **I**, determined by plotting loss of EPR signal versus time after extinguishing the UV light, shows an initial decay of less than 10% of the signal intensity within 20 s after extinguishing the UV light and no further significant decay after 4 min. (iii) The UV light intensity and instrument settings were kept constant throughout each series of experiments.

The slow growth of **I** over a time period of minutes for $NaNO_2$ solutions contributed to quantitative measurements, because this allowed sufficient time to record the EPR spectra without resorting to rapid scan sweeps. We estimate that for a typical set of EPR spectra of **I** the standard deviation of the spin concentrations determined by integration methods is $s = 3.7 \times 10^7$ spins and the variance is $s^2 = 1.4 \times 10^{15}$ spins.[14] For a normal distribution, this gives a probable error of standard deviation of $\sigma = 0.674\ s$ or 2.4×10^7, which gives a probable error of variance of $\pm 0.6 \times 10^{15}$ spins.

As stated in the Introduction, the goal of these experiments is to provide a spin trapping method of measuring the concentration of nitrite ions from photodecomposition of nitramines in basic alkaline solution, thereby estimating the extent of photodecomposition of each nitramine. For example, for the solution of RDX, the NO_2^- concentration determined from the calibration plot (Figure 7b) is ca. 40×10^{-3} mol L^{-1}. If 2 mol of NO_2^- is produced per mole of RDX, as has been suggested at high pH, this gives an RDX concentration of 20×10^{-3} mol L^{-1}.[3] In this experiment 1.7×10^{-4} mol of RDX was added to 3 mL of basic solution, but only a fraction of this amount dissolved initially. The results suggest that 20×10^{-3} mol $L^{-1} \bullet 3 \times 10^{-3}$ L $= 6 \times 10^{-5}$ mol of RDX decomposed in solution. This gives a mole fraction of 0.35 of the RDX (1.7×10^{-4} mol) which decomposed in solution.

In preliminary experiments we have observed that the addition of a catalyst, such as TiO_2, can enhance the decomposition of nitramines in alkaline solution. The nitromethane spin trapping method might enable simultaneous determination of the extent of decomposition of nitramines and the effectiveness of added catalysts.

Summary

EPR spin trapping with *aci*-nitromethane is demonstrated as a quantitative technique for estimating nitrite ion concentrations in strong alkaline aqueous solutions. The method was applied to solutions of sodium nitrite to produce plots of radical adduct [$^-NO_2-CH{=}NO_2^{\bullet -}$] concentration versus time of photolysis or nitrite ion concentration. The photochemical decomposition of cyclotrimethylenetrinitramine was estimated based on the nitrite ion concentration determined by the *aci*-nitromethane method. For ADN, 1.4 NO_2^- ions were estimated to form per molecule of ADN in alkaline solution when exposed to UV light. This method of estimating nitrite ion concentrations may be used to study catalytic enhancement of decomposition of energetic materials.

Acknowledgment. Support for this research was provided by the Office of Naval Research, Arlington, VA. Assistance of Dr. K. Swider, a Naval Research Laboratory postdoctoral associate, is acknowledged for preliminary data involving catalysts.

References and Notes

(1) Urbanski, T. *Chemistry and Technology of Explosives*; Pergamon Press: London, 1965; Vol. 2.

(2) Hoffsommer, J. C.; Kubose, D. A.; Glover, D. J. *J. Phys. Chem.* **1977**, *81*, 380−387.

(3) Glover, D. J.; Hoffsommer, J. C. Photolysis of RDX in aqueous solution. Naval Surface Warfare Center, Report NSWC/WOL TR 78-175, 1979 (unclassified).

(4) Snell, F. D.; Snell, T. C. *Colorimetric Measurements of Analysis*; Van Nostrand: Princeton, NJ, 1949; pp 785−807.

(5) Walter, T. H.; Bancroft, E. E.; McIntire, G. L.; Davis, E. R.; Gierasch, L. M.; Blount, H. N.; Stronks, H. J.; Janzen, E. G. *Can. J. Chem.* **1982**, *60*, 1621−1636.

(6) A preliminary account of this research was published in the Proceedings of Life Cycles of Energetic Materials II, Del Mar, CA, Dec 1994.

(7) Pace, M. D. *J. Phys. Chem.* **1994**, *98*, 6251−6257.

(8) Gilbert, B. C.; Norman, R. O. *Can. J. Chem.* **1982**, *60*, 1379−1391.

(9) Bilski, P.; Chignell, C. F.; Szychlinski, J.; Borkowski, A.; Olesky, E.; Reska, K. *J. Am. Chem. Soc.* **1992**, *114*, 549−556.

(10) Reszka, K. J.; Chignell, C. F.; Bilski, P. *J. Am. Chem. Soc.* **1994**, *116*, 4119−4120.

(11) SUMSPEC is a computer program for EPR spectral manipulation and analysis written and distributed by the Biophysics Research Institute, Medical College of Wisconsin, Milwaukee, WI.

(12) Krzysztof, J.; Reska, C. F.; Chignell, C. F. *J. Photochem. Photobiol.* **1994**, *60*, 442−449.

(13) Moore, D. E.; Sik, R. H.; Bilski, P.; Reszka, K. J.; Chignell, C. F. *Photochem. Photobiol.* **1994**, *60*, 574−581.

(14) Crow, E. L.; Davis, F. A.; Maxfield, M. W. *Statistics Manual*; Dover Publications: New York, 1960.